European Journal of Medicinal Chemistry xxx (xxxx) 113693

Contents lists available at ScienceDirect

European Journal of Medicinal Chemistry

journal homepage: www.elsevier.com/locate/ejmech

Structure-based screening for the discovery of 1,2,4-oxadiazoles as promising hits for the development of new anti-inflammatory agents interfering with eicosanoid biosynthesis pathways

Marianna Potenza [a, b, 1], Martina Sciarretta [c, 1], Maria Giovanna Chini [d], Anella Saviano [c], Francesco Maione [c], Maria Valeria D'Auria [c], Simona De Marino [c], Assunta Giordano [a, e], Robert Klaus Hofstetter [b], Carmen Festa [c, **], Oliver Werz [b], Giuseppe Bifulco [a, *]

[a] Department of Pharmacy, University of Salerno, Via Giovanni Paolo II, 132, 84084, Fisciano, Italy
[b] Department of Pharmaceutical/Medicinal Chemistry, Institute of Pharmacy, Friedrich Schiller University Jena, Philosophenweg 14, 07743, Jena, Germany
[c] Department of Pharmacy, University of Naples, Via Domenico Montesano, 49, Naples, 80131, Italy
[d] Department of Biosciences and Territory, University of Molise, Contrada Fonte Lappone, Pesche, Isernia, I-86090, Italy
[e] Institute of Biomolecular Chemistry (ICB), Consiglio Nazionale Delle Ricerche (CNR), Via Campi Flegrei 34, I-80078, Pozzuoli, Napoli, Italy

ARTICLE INFO

Article history:
Received 21 May 2021
Received in revised form 6 July 2021
Accepted 7 July 2021

Keywords:
Combinatorial chemistry
Oxadiazoles
Eicosanoid biosynthesis pathways
Polypharmacology
Anti-inflammatory activity

ABSTRACT

The multiple inhibition of biological targets involved in pro-inflammatory eicosanoid biosynthesis represents an innovative strategy for treating inflammatory disorders in light of higher efficacy and safety. Herein, following a multidisciplinary protocol involving virtual combinatorial screening, chemical synthesis, and *in vitro* and *in vivo* validation of the biological activities, we report the identification of 1,2,4-oxadiazole-based eicosanoid biosynthesis multi-target inhibitors. The multidisciplinary scientific approach led to the identification of three 1,2,4-oxadiazoles hits (compounds **1**, **2** and **5**), all endowed with IC_{50} values in the low micromolar range, acting as 5-lipoxygenase-activating protein (FLAP) antagonists (compounds **1** and **2**), and as a multi-target inhibitor (compound **5**) of arachidonic acid cascade enzymes, namely cyclooxygenase-1 (COX-1), 5-lipoxygenase (5-LO) and microsomal prostaglandin E_2 synthase-1 (mPGES-1). Moreover, our *in vivo* results demonstrate that compound **5** is able to attenuate leukocyte migration in a model of zymosan-induced peritonitis and to modulate the production of IL-1β and TNF-α. These results are of interest for further expanding the chemical diversity around the 1,2,4-oxadiazole central core, enabling the identification of novel anti-inflammatory agents characterized by a favorable pharmacological profile and considering that moderate interference with multiple targets might have advantages in re-adjusting homeostasis.

1. Introduction

In the last years, several studies have reported the importance of prostaglandin E_2 (PGE_2) in the evolvement and progression of inflammatory and tumor diseases and the implication of the interference with this lipid mediator as a therapeutic strategy [1,2]. Interestingly, this paved the way for investigations concerning the effects of inhibition of PGE_2 biosynthesis on the aforementioned pathological conditions [2]. PGE_2 is synthesized in stimulated cells starting from arachidonic acid (AA), released from cellular membranes by cytosolic phospholipase A_2 ($cPLA_2$) for triggering the inflammatory cascade. Specifically, AA can be converted to pro-inflammatory mediators by at least three different pathways (Fig. 1), namely a) cyclooxygenases pathway for the synthesis of prostanoids, b) 5-lipoxygenase (5-LO) pathway for the synthesis of leukotrienes, c) CYP450 pathway for the synthesis of dihydroxyeicosatrienoic acids (DHETs). Microsomal prostaglandin E_2 synthase-1 (mPGES-1) [3] is an enzyme belonging to the prostanoid biosynthetic pathway (Fig. 1) involved in the conversion of the unstable PGH_2 into PGE_2, and its activity is coupled to the inducible isoform of cyclooxygenases (i.e. COX-2) [2,3]. In fact, mPGES-1 has been identified as a promising target for the treatment of both inflammation [4] and tumor diseases [5–7]. Several pharmacological investigations reported an up-regulation of mPGES-1 induced by IL-1β, LPS, TNF-α, and other inflammatory stimuli [6,8,9] and a connection between the concentration of

* Corresponding author.
** Corresponding author.
E-mail addresses: carmen.festa@unina.it (C. Festa), bifulco@unisa.it (G. Bifulco).
[1] These authors contributed equally to this work.

https://doi.org/10.1016/j.ejmech.2021.113693
0223-5234/

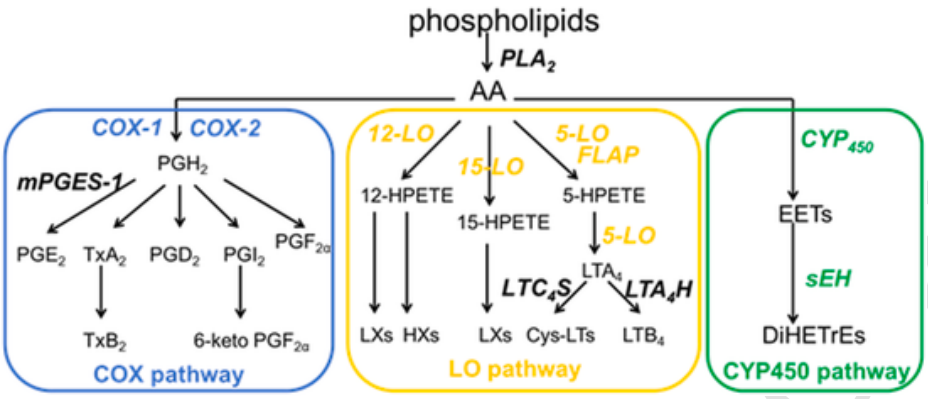

Fig. 1. Three different branches for the biosynthesis of inflammation mediators starting from arachidonic acid (AA).

PGE_2 and cancer progression [10]. Contrariwise, the cytosolic cPGES and the microsomal mPGES-2 are constitutively expressed isoforms [11] involved in physiological functions and organ homeostasis. mPGES-1 is a membrane protein consisting of 152 amino acids organized as a homotrimer, with each monomer formed by four transmembrane helices (namely TM1-TM4), and containing a catalytic binding site between the N-terminal parts of TM2 and TM4 and the C-terminal part of TM1 and the cytoplasmic domain of the adjacent monomer. It belongs to the MAPEG (Membrane-Associated Proteins involved in Eicosanoid and Glutathione metabolism) superfamily, together with the 5-LO-activating protein (FLAP), leukotriene C4 synthase (LTC_4S), and microsomal glutathione S-transferases [12]. Several mPGES-1 inhibitors derive from compounds that interfere with proteins belonging to MAPEG, such as from FLAP antagonists like MK886 [13,14].

Considering that mPGES-1 is placed downstream in the prostanoid biosynthetic pathway (Fig. 1), different classes of mPGES-1 inhibitors have been identified up to now [15–19], with the primary purpose of disclosing novel chemical entities for the treatment of inflammation avoiding the well-known side effects of COX inhibitors. However, there is a strong interconnection between the three branches of AA cascade, where treatment with drugs selectively targeting one branch is frequently coupled to several side effects deriving from the consequences on the entire AA cascade due to shunting phenomena.

Interestingly, multi-target strategies have been recently adopted in order to amplify the desired anti-inflammatory effects and provide a solution to the side effects deriving from the single-target selectivity [20], considering that the moderate interference with multiple targets might have advantages compared to single-target drugs in re-adjusting homeostasis [21]. In light of these considerations, dual mPGES-1/FLAP [13,14] or mPGES-1/5-LO [22,23] inhibitors have been developed in the last years. In this context, here we report the application of a multidisciplinary approach towards the identification of 1,2,4-oxadiazoles as anti-inflammatory agents. Compounds **1**, **2** and **5** were discovered as novel potent chemical items modulating the eicosanoid biosynthesis pathways, with compound **5** presenting multi-target activity, interfering at different levels within the arachidonic acid cascade, both horizontally and vertically in the COX and 5-LO pathways (specifically COX-1, 5-LO and mPGES-1; Fig. 1). Finally, *in vivo* and *ex-vivo* analyses support the pharmacological effects of **5**, which displays bioactivity in the acute phase of a mouse model of zymosan-induced peritonitis.

2. Results and discussion

2.1. Combinatorial approach

In this study, a multidisciplinary approach was applied with the main purpose of identifying novel promising anti-inflammatory chemical entities, mainly focused on interfering mPGES-1 activity. Specifically, the applied methodologies were well-linked and connected to each other, with each step being a consequence of the previous one. The selection of 1,2,4-oxadiazole as a chemical feature to focus on was the first step of the workflow in our study. Oxadiazoles, in fact, show high incidence among pharmacologically active compounds, covering a broad biological activity spectrum, such as antihypertensive, analgesic, antiviral, anticancer, anticonvulsant, antidiabetic, anti-inflammatory [24,25]. Especially, the 1,3,4-oxadiazole core is widespread among pharmacological agents [24–29]. On the other hand, many 1,2,4-oxadiazole-containing compounds showed anti-inflammatory activity [30] acting as NF-κB inhibitors [31], or modulating eicosanoid enzymatic pathways (COX, 5-LO or FLAP inhibitors) [31–35], however their inhibitory activity on mPGES-1 was yet not explored.

The two most common routes for the synthesis of 1,2,4-oxadiazoles are the 1,3-dipolar cycloaddition of nitriles to nitrile *N*-oxides and the cyclization of amidoxime derivatives. In this context, the *O*-acylation of amidoximes by carboxylic acids, followed by cascade cyclization-dehydration, appears the most versatile approach. This synthetic scheme offers the advantage of the high modularity of the process due to the commercial availability of a wide variety of nitriles and carboxylic acids, providing 1,2,4-oxadiazole products bearing different substituents at positions 3 and 5. Thus, starting from these premises, 1,2,4-oxadiazole was decorated with side chains (R_1 and R_2) of 55 nitriles and 4888 carboxylic acids (Fig. 2) respectively, available at Merck database, using CombiGlide software [36,37], to obtain a final library of 273,728 novel compounds.

Then, after the generation of all tautomers and ionization states at physiological pH (LigPrep software) [38], QikProp software [39] was used to calculate the pharmaceutically relevant properties of the designed molecules. Among them, the number of violations of Lipinski's rule of five (namely, mol_MW < 500, QPlogPo/w < 5, donorHB ≤ 5, accptHB ≤ 10, see experimental section and Table S1, Supporting Information) was used for firstly filtering the combinatorial library discard-

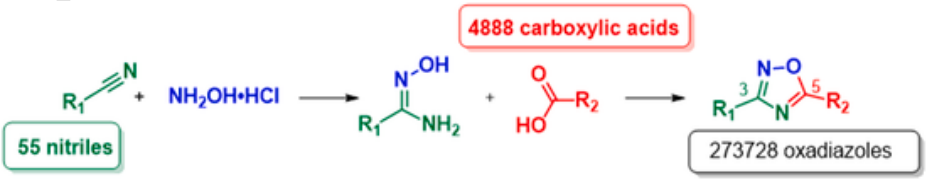

Fig. 2. Generation of the novel library of 1,2,4-oxadiazoles using Combiglide software.

ing, in this way "non-drug like" compounds. Then, a final library of 150,512 molecules was submitted to the successive virtual screening workflow (VSW) on mPGES-1 (pdb code: 5TL9) [40] using Glide [41] software. In more detail, the VSW was employed following three subsequent steps: a) High-Throughput Virtual Screening (HTVS) phase; saved the top 60% of compounds ranked by docking score for the subsequent step; b) Standard Precision phase (SP); saved the top 60% of compounds ranked by docking score for the subsequent step; c) Extra Precision phase (XP), saved the top 70% of compounds ranked by docking score. The binding mode of the filtered compounds was investigated by analyzing the related docking poses and checking the establishment of specific sets of interactions responsible for mPGES-1 inhibitory activity in the binding sites, delimited by polar, charged, aliphatic and aromatic residues ($Val24_{ChainC}$, $Tyr28_{ChainC}$, $Phe44_{ChainC}$, $Arg52_{ChainC}$, $His53_{ChainC}$, $Pro124_{ChainA}$, $Ser127_{ChainA}$, $Val128_{ChainA}$, $Tyr130_{ChainA}$, $Thr131_{ChainA}$, $Leu132_{ChainA}$, $Gln134_{ChainA}$). The application of several filters like the selection of the most affine poses by docking score, the analysis of the key ligand-protein interactions required for the inhibition reported by us [15–18] and other groups [35,42–46], and the final visual inspection, led to the selection of a small library of eleven compounds (**1**–**11**, Fig. 3) characterized by a common 4-(thiophen-3-yl)phenyl substitution at position 3 and variable 5-substitution on the 1,2,4-oxadiazole ring.

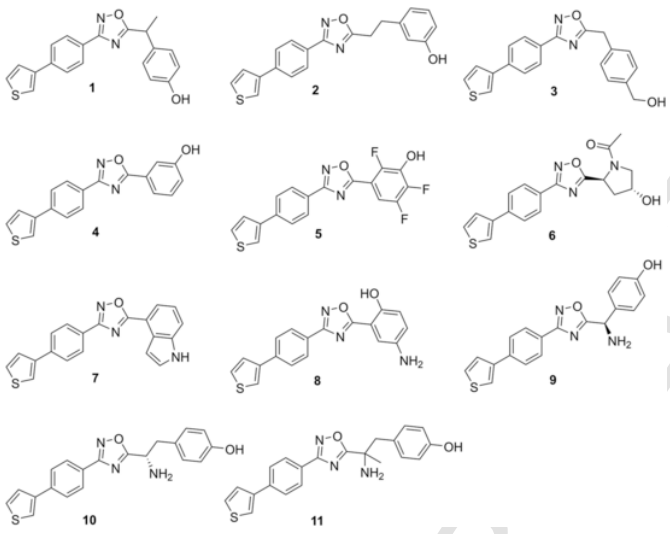

Fig. 3. Selected compounds 1–11 for the synthesis.

Before proceeding with the successive synthetic stage, the selected compounds were further analyzed by SwissADME [47], for filtering the compound displaying the features of "Pan-Assay Interference Compounds", and by detailed analysis of the other specific pharmaceutically relevant properties (QikProp software, see experimental section and Table S1, Supporting Information) related to: i) absorption, distribution, metabolism, and excretion (ADME) (e.g., QPlogPo/w); ii) types of reactive functional groups that may cause false positives in high-throughput screening (HTS) assays, and/or decomposition, reactivity, or toxicity problems *in vivo* (#rtvFG and #metab parameters in,Table S1 Supporting Information). Thanks to these computational predictions, the most promising compounds showing a good equilibrium between chemical diversity around the 1,2,4-oxadiazole ring central core, docking score, qualitative target interactions, and pharmacokinetic properties were selected for the successive experimental steps.

2.2. Synthesis of compounds *1*–*11*

Compounds **1–11** were synthesized following the chemical route reported in Scheme 1. In particular, the oxadiazole moiety was prepared from nitrile **12** through the formation of N-hydroxyimidamide intermediate **13**, followed by a one-pot cyclization with different carboxylic acids, using HBTU as coupling reagent and Hu¨nig's base, to afford the target compounds **1–7** (Scheme 1). For compounds **8**–**11**, Boc-protected acids (**8a-11a**) were used and then the corresponding oxadiazole derivatives **8b**–**11b**, subjected to the deprotection with TFA in DCM, afforded the final compounds **8–11**.

The structure of the synthesized compounds was confirmed by analysis of NMR data (^1H, ^{13}C and bidimensional NMR spectra) and ESI-MS (see Experimental section and Supplementary data).

2.3. Biological evaluation

2.3.1. Enzyme inhibition

A cell-free bioactivity assay [48] was used to screen all the synthesized compounds for mPGES-1 inhibition. All the compounds were tested at 10 μM, and compound **5** was able to reduce the enzyme activity by approx. 75% versus vehicle control (Table 1). A concentration-response analysis was then performed, testing compound **5** at different concentrations (from 0.03 μM up to 10 μM, Fig. 4). Interestingly, compound **5** displayed an IC_{50} value at the low micromolar range (IC_{50} = 3.6 ± 0.7 μM) for mPGES-1. Thus, the 3-hydroxy-2,4,5-

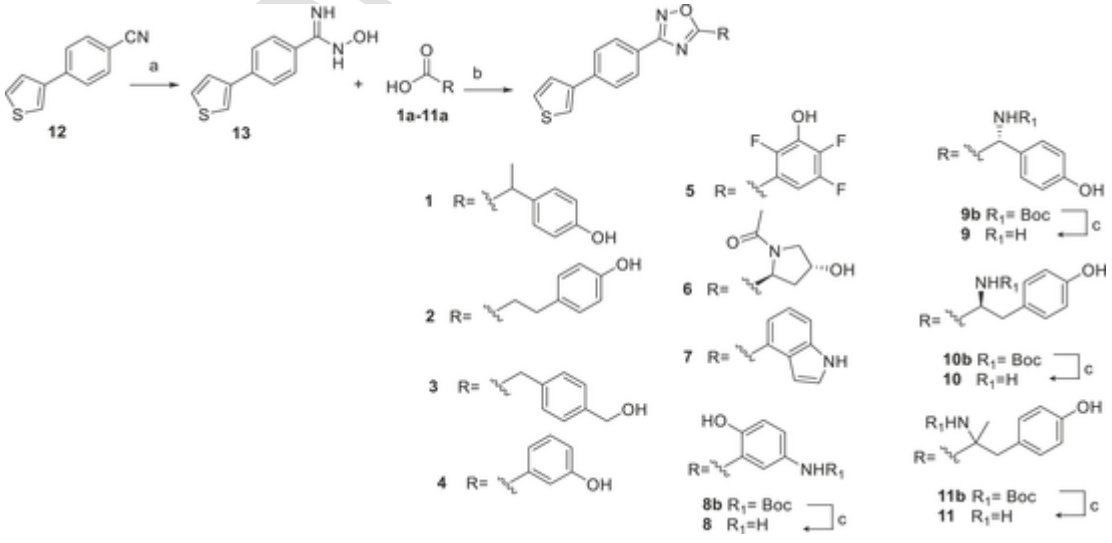

Scheme 1. Synthesis of compounds 1–11.[a].

trifluorophenyl substituent was identified as the chemical key for interference with mPGES-1.

Considering the similarity in the structure of mPGES-1 and FLAP, both belonging to the MAPEG superfamily [13,14], all the compounds were screened at 10 μM for inhibition of FLAP-dependent 5-LO product (LTB_4 and its isomers, and 5-H(p)ETE) formation in human intact neutrophils isolated from human peripheral blood. FLAP is proposed to provide arachidonic acid as a substrate to 5-LO but no enzymatic activity of FLAP is yet known and thus, a direct FLAP activity assay (cell-free or cell based) is not available. To investigate antagonism of FLAP, the compounds were tested in neutrophils where Ca^{2+}-ionophore was used to elicit 5-LO product formation, while exogenous addition of arachidonic acid largely circumvents the requirement of FLAP [49]. Interestingly, after neutrophils were incubated with compounds **1**, **2** and **5**, a reduction of 5-LO product formation by more than 50% in comparison to the vehicle control (100%) was found for all these three compounds, with **5** showing the most potent effects, especially in the absence of exogenous arachidonic acid (Table 1).

At this point, a cell-free 5-LO activity assay was performed with compounds **1**, **2** and **5** in order to study if the compounds possess direct inhibitory effects on 5-LO. Compounds **1** and **2** showed only poor inhibitory activity against 5-LO (Table 2), thus suggesting that suppression of 5-LO product formation in neutrophils might be due to interference with FLAP. However, compound **5** potently blocked 5-LO activity in the cell-free assay with an IC_{50} value in the micromolar range (IC_{50} = 2.0 ± 0.2 μM), indicating that inhibition of 5-LO and/or FLAP may account for the suppression of 5-LO product formation by compound **5** in intact cells.

Additionally, compounds **1**, **2** and **5** were screened against soluble epoxide hydrolase (sEH) with the main purpose of identifying additional targets in order to investigate and strengthen their anti-inflammatory properties. Compounds **1**, **2** and **5** showed no inhibitory activity (Table 2) against sEH in a cell-free assay. Finally, a cell-free assay was performed also for analysis of COX-1 and COX-2. Interestingly, compounds **1** and **5** were able to reduce the activity of COX-1 by >65% compared to control (100%), and also compound **2** inhibited COX-1 by >50%, but no activity of any of these three compounds was found on the inducible isoform COX-2, which acts together with mPGES-1. Considering that only few COX-1-selective inhibitors have been developed, the selectivity of compound **1**, **2** and **5** for this isoform may be of interest for future findings. Recent studies, in fact, reported an involvement of COX-1 in neoplastic diseases, such as renal carcinoma, skin, esophageal and colorectal, breast, endometrial, ovarian cancers [50].

Finally, compounds **1**, **2** and **5** were tested in cytotoxicity assays. The compounds showed no significant reduction of cell viability after 24 h incubation in human monocytes compared to triton (positive control), and, moreover, no reduction of cell viability after 48 h incubation with the human adenocarcinoma A549 cell line was observed for **5** (Fig. 5).

Considering the biological evaluation reported above, the detailed description of the ligand/target interactions between mPGES-1 and compound **5** was chosen as a representative case to elucidate the structural basis responsible for enzyme inhibition at the molecular level (Fig. 6). In particular, the 1,2,4-oxadiazole moiety centers the binding site, placing in proximity to the glutathione interacting space of the enzyme. The phenyl moiety at position 3 establishes π-π interactions with $Tyr130_{chainC}$. The thiophene ring is involved in π-π interactions with $Tyr130_{chainC}$ and $Tyr28_{chainA}$ orienting towards the key residue $Gln134_{chainC}$. On the other side, the hydroxytrifluorophenyl substituent interacts with the cytoplasmic part of the ligand binding site, i.e., establishing π-π interactions with $His53_{chainA}$ and H-bonding to $Ser127_{chainC}$ with the hydroxyl group.

From a structural point of view, the mPGES-1 inhibitory activity of **5** with respect to the other compounds of this series, e.g., to its linked congener (**4**), is ascribable to the presence of the hydroxypolyfluorinated phenyl substituent, which also interacts with the $Arg52_{chainA}$.

The electronic properties and relatively small size of the fluorine atom in fact, endow it with considerable versatility as a bioisoster of several functional groups [51] in drug design.

Among all the possible *m*-hydroxy-polyfluorinated phenyl analogues (see Figures S12-S21, Supporting Information for their *in silico* models), thanks to this type of experimental workflow, we have selected only the items that could be representative of a specific ligand/target interaction pattern: the influence of fluorine substitution in two opposite cases (**4** vs. **5**) on mPGES-1 inhibitory potency, paving the way to future optimization.

The obtained results are of interest for further expanding the chemical diversity around the 1,2,4-oxadiazole central core, facilitating the identification of novel anti-inflammatory agents endowed with a promising and safer pharmacological profile.

Table 1
Inhibition of compounds **1**–**11** on mPGES-1 activity and 5-LO product formation.

Compd.	R	Residual activity of mPGES-1 (%) ± SEM[a]	Residual 5-LO product (%) *Stimulus*: A23187[b]	Residual 5-LO product (%) *Stimulus*: A23187 plus AA[b]
1	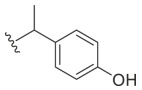	62.9 ± 5.6	6.02	7.54
2	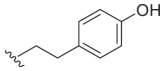	76.4 ± 2.7	19.9	14.9
3	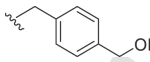	93.1 ± 5.7	73.6	65.2
4	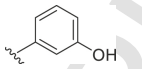	84.1 ± 7.8	n.i. (> 100%)	n.i. (> 100%)
5	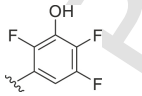	25.4 ± 2.7	1.7	18.5
6	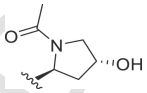	82.2 ± 7.5	92.6	89.5
7	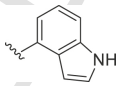	63.2 ± 10.1	59.7	99.3
8	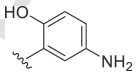	81.9 ± 8.1	84.3	29.6
9	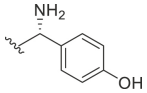	67.6 ± 2.1	47.5	50.3
10	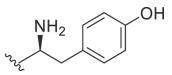	82.7 ± 8.7	95	74.4
11	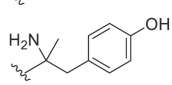	84.7 ± 5.8	78	61.3

[a] mPGES-1 residual activity of compounds **1–11** deriving from the cell-free assay. Data are expressed as percentage of control (100%) ± S.E.M., n = 3.

[b] 5-LO product formation in intact human neutrophils after incubation with compounds **1–11**. *Stimulus*: A23187 or A23187 plus arachidonic acid (AA). Data are expressed as percentage of control (100%).

[a] *Reagents and conditions*: a) NH_2OH HCl, K_2CO_3 in CH_3OH, reflux, 70% yield; b) Acids **1a-11a**, DIPEA, HBTU in DMF dry, 80 °C, 40–75% yield; c) TFA:CH_2Cl_2 1:1, 2 h, quantitative yield.

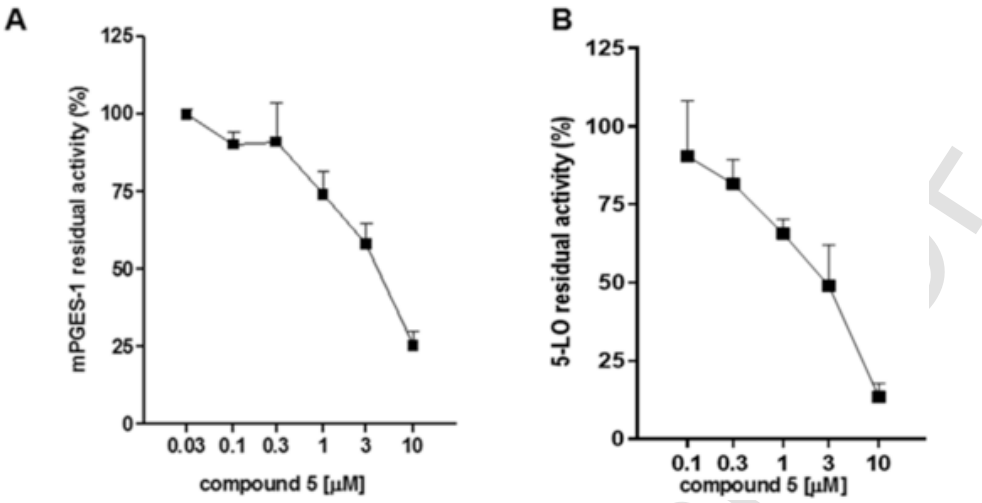

Fig. 4. A) Concentration-response curve for inhibition of mPGES-1. The enzyme was incubated for 15 min with compound **5** at different concentrations (from 0.03 μM up to 10 μM) or vehicle (1% DMSO). Then, 20 μM PGH_2 was added as substrate, and the reaction was stopped after 1 min by adding $FeCl_3$. IC_{50} = 3.6 ± 0.7 μM. **B**) Concentration-response curve of compound **5** for 5-LO inhibition in a cell-free assay. The purified 5-LO enzyme was pre-incubated 10 min on ice with compound **5** at different concentrations or vehicle (0.1% DMSO). Then, AA (20 μM) and $CaCl_2$ (2 mM) were added, and the mixture was incubated at 37 °C. After 10 min, the reaction was stopped by adding ice-cold methanol. IC_{50} = 2.0 ± 0.2 μM. Data are expressed as percentage of control (100%), means ± S.E.M.; n = 3.

Table 2
Residual activity of compounds **1**, **2** and **5** at 10 μM on isolated enzymes involved in the formation of pro-inflammatory eicosanoids. Data are expressed as a percentage of control (100%), n = 3.

Compd.	5-LO residual activity (%)	sEH residual activity (%)	COX-1 residual activity (%)	COX-2 residual activity (%)
1	n.i (61.8)	n.i. (>50)	22.5	n.i. (>50)
2	n.i. (104.8)	n.i. (>50)	47.7	n.i. (>50)
5	10.3	n.i. (>50)	34.7	n.i. (>50)

2.3.2. *In vivo and ex vivo assays*

Based on the results obtained from *in vitro* experiments, we next investigated the effects of compound **5** in an *in vivo* model of inflammation that allows the characterization of leukocytes egress into the peritoneal cavity. Zymosan, a polysaccharide cell wall component derived from *Saccharomyces cerevisiae*, has been reported to elicit a multiple organ failure and a massive recruitment of innate immunity cells in the peritoneal cavity, mainly characterized by neutrophils and monocytes recruitment [52]. We know from previous studies that a single administration of zymosan into the peritoneal cavity causes a transient infiltration of leukocytes that becomes evident between 4 and 24 h, and then declines at 48 h.[53-56] Mice were subjected to i.p. injection of 500 mg/kg zymosan, in the presence or absence of compound **5** (0.1–10 mg/kg dissolved in DMSO/saline 1:3 and given i.p. 30 min after zymosan). As an internal control, i.p. injection of PBS alone without zymosan and i.p. injection of dexamethasone (3 mg/kg) 30 min post zymosan administration were also assessed.

As shown in Fig. 7A, zymosan injection elicits at 4 h a strong leukocyte recruitment that was significantly reduced by compound **5** administration at the dose of 10 mg/kg ($P \leq 0.01$). Conversely, after 24 h (Fig. 7B), the anti-inflammatory effect of compound **5** was less evident ($P \leq 0.05$) compared to zymosan + vehicle compound **5** group. Interestingly, compound **5** displayed a significant effect even at the lower dose of 1 mg/kg ($P \leq 0.05$) at the 4 h time-point (Fig. 7A). The refer-

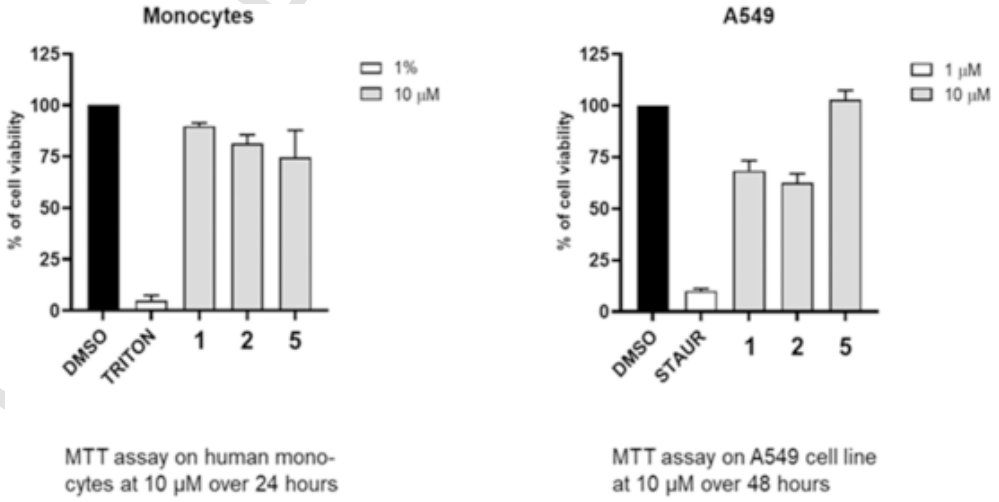

Fig. 5. Cell viability assays were performed with human monocytes and A549 cells. **A**) Monocytes were treated with the test compounds **1**, **2** and **5** (10 μM), triton (1%, positive control) or vehicle (0.5% DMSO) for 24 h, and a MTT assay was performed; **B**) A549 cells were treated with the test compounds **1**, **2** and **5** (10 μM), staurosporine (1 μM, positive control) or vehicle (0.1% DMSO) for 48 h, and a MTT assay was performed. Data are expressed as percentage of control (100%), means, S.E.M., n = 3.

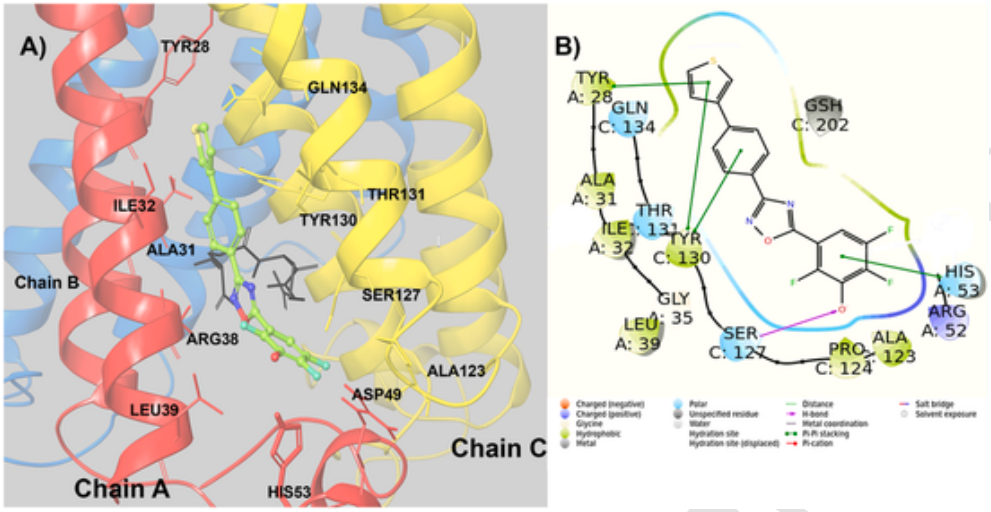

Fig. 6. A) 3D representation of compound **5** (green sticks) in the binding site of mPGES-1 (pdb code: 5TL9); chain A is depicted in yellow, chain B in blue, and chain C in red ribbons; all the interactions are represented as dotted lines, green in hydrogen bonds, light blue in π-π interactions. **B)** 2D interactions diagram of compound **5** with mPGES-1 as counterpart (pdb code: 5TL9); H-bond interactions are reported as pink arrows, while π-π interactions as green lines; hydrophobic residues are depicted in green, polar residues in light blue, and positive charged residues in blue.

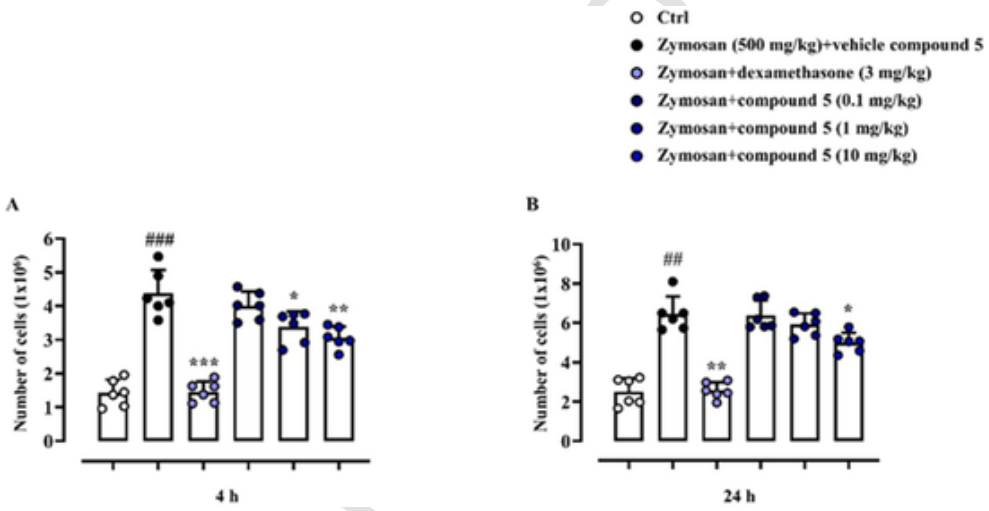

Fig. 7. Effect of compound **5** in zymosan-induced peritonitis in mice. Mice were randomly divided into different experimental groups: control group (Ctrl), model group (zymosan + vehicle compound **5**), zymosan + compound **5** (0.1, 1, and 10 mg/kg), and zymosan + dexamethasone (3 mg/kg) group. Animals received the selected compound or dexamethasone intraperitoneally (i.p.) 30 min after i.p. injection of zymosan (500 mg/kg). **A)** At 4 and **B)** 24 h after injection, peritoneal exudate from each mouse was recovered and total cell number (expressed as 10^6 and normalized to exudate levels) was evaluated. Results are expressed as mean ± S.D. Statistical analysis was performed by using one-way ANOVA followed by Bonferroni's for multiple comparisons. $^{\#\#}P \leq 0.01$ and $^{\#\#\#}P \leq 0.005$ *vs* Ctrl group, $^{*}P \leq 0.05$, $^{**}P \leq 0.01$ and $^{***}P \leq 0.005$ *vs* zymosan + vehicle compound **5**-treated mice (n = 6 per group).

ence drug dexamethasone was able to significantly reduce leukocyte numbers in the peritoneal cavity at both 4 ($P \leq 0.005$;Figs. 7A) and 24 h ($P \leq 0.01$; Fig. 7B).

Consistently with our previous findings, 4 and 24 h after a single injection of zymosan (500 mg/kg) i.p there was a significant increase in the levels of IL-1β (Fig. 8A and B), TNF-α (Fig. 8C and D), and IL-6 (Fig. 8E and F) compared to the Ctrl group (without zymosan). Conversely, IL-10 levels were significantly reduced at both time points (Fig. 8G and H). Interestingly, compound **5** at 10 mg/kg significantly reduced the levels of IL-1β (Fig. 8A and B; $P \leq 0.01$ and $P \leq 0.05$ at 4 and 24 h respectively) and TNF-α (Fig. 8C and D; $P \leq 0.05$ at both 4 and 24 h) without altering the level of IL-6 and IL-10 (Fig. 8*E*–H). Injection of dexamethasone (3 mg/kg) decreased the values of IL-1β, TNF-α and IL-6 with a more prominent effect (Fig. 8A–F).

The role of pro-inflammatory cytokines, such as IL-1β, IL-6, TNF-α and PGs with consequent cellular infiltration and exudate formation is well established in the pathophysiology of zymosan-induced inflammation and shock [53–55]. TNF-α plays a pivotal role characterized by the earliest and large releases in a short time followed by IL-1 and IL-6 that orchestrate neutrophils, macrophages, and fibroblasts accumulation to the site of inflammation [56,57]. On the other hand, IL-10 is an anti-inflammatory cytokine that mainly suppresses inflammatory response inhibiting the activation and function of T cells and monocytes [58–60]. Our results demonstrate that the zymosan-induced leukocytes migration was attenuated by treatment with compound 5, starting from 4 h post model induction. Furthermore, the screening of the main pro-inflammatory cytokines showed a significant reduction in the levels of IL-1β and TNF-α by compound 5 but not modulation in terms of IL-6 and IL-10 production. The difference in leukocytes accumulation and cytokines level observed between 4 and 24 h (even compared to the reference drug dexamethasone) may be due to the route of administration and compound's bioavailability. To assess this possibility, further animal studies will be carried out using other *in vivo* models as well other structural compound 5 analogues/derivates.

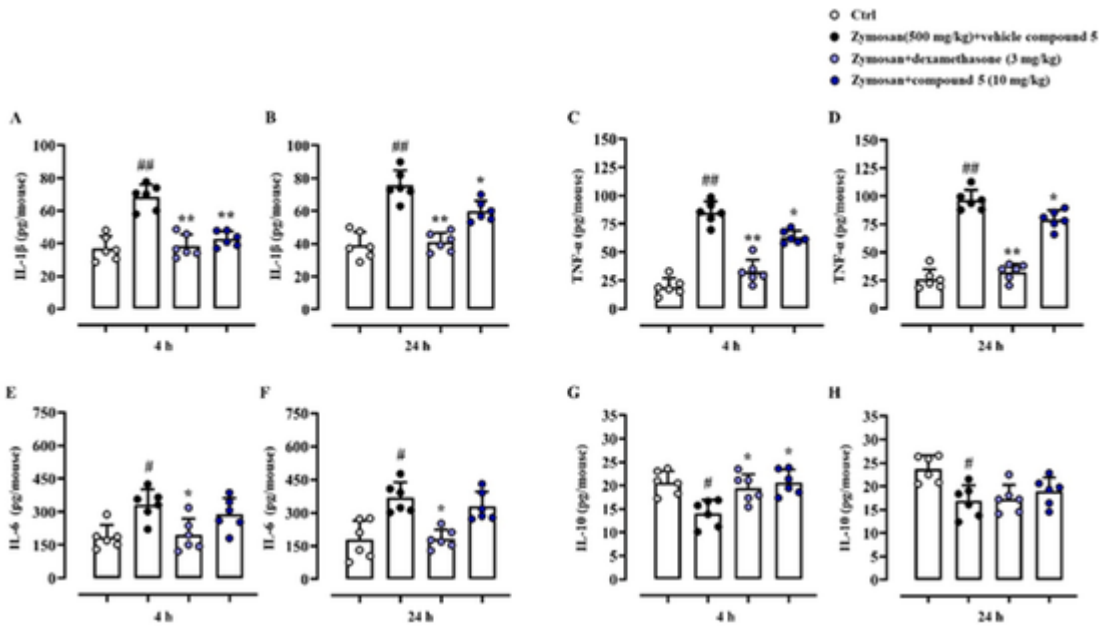

Fig. 8. Cytokines analysis of the collected peritoneal exudate. Analysis of the collected peritoneal exudate identified increased levels of the classical pro-inflammatory mediators **A**,**B**) IL-1β, **C**,**D**) TNF-α, **E**,**F**) IL-6, and decreased of **G**,**H**) IL-10 in the peritoneal cavity of mice from different experimental groups. Significant differences were found in relative levels after compound **5** administration. Results (normalized to exudate levels) are expressed as mean ± S.D. Statistical analysis was performed by using one-way ANOVA followed by Bonferroni's for multiple comparisons. $^{\#}P \leq 0.05$ and $^{\#\#}P \leq 0.01$ *vs* Ctrl group, $^{*}P \leq 0.05$ and $^{**}P \leq 0.01$ *vs* zymosan + vehicle compound **5** treated mice (n = 6 per group).

3. Conclusions

In this study, the application of a multidisciplinary approach consisting of well-linked experimental steps is reported as a powerful tool towards the identification of novel pharmacologically active compounds. In this context, a multistep computational protocol coupled to a versatile synthetic approach and a fast biological screening on several lipid mediator biosynthetic enzymes involved in the progression of inflammation led to the disclosure of 1,2,4-oxadiazole derivatives, compounds **1**, **2** and **5**, as new potent anti-inflammatory chemical items. In particular, compound **5** is able to interfere with the biosynthesis of prostanoids and leukotrienes, exhibiting a horizontally and vertically multi-target inhibitory activity on both COX and 5-LO pathways (COX-1, mPGES-1, and 5-LO) with IC_{50} values at the low micromolar range. Compounds **1** and **2** inhibited 5-LO product formation in human neutrophils seemingly acting on FLAP. Interestingly, besides inhibiting mPGES-1, compound **5** was able to inhibit the activity of COX-1, paving the way to future deeper pharmacological investigations. Thus, opportunely decorated 1,2,4-oxadiazole proved to be a promising scaffold for the identification of pharmacologically active compounds, especially for the treatment of inflammatory pathologies related to eicosanoids. Moreover, our *in vivo* results demonstrate that compound **5** is able to attenuate leukocytes migration in a model of zymosan-induced murine peritonitis and to modulate the production of IL-1β and TNF-α. However, further studies will be necessary to better characterize the complete anti-inflammatory profile of compound **5** and/or its analogues/derivatives. In light of the encouraging preliminary outcomes, the application of our multidisciplinary approach may lead us to an optimization campaign with the aim of identifying novel 1,2,4-oxadiazoles derivatives with strong anti-inflammatory properties.

4. Experimental

4.1. Computational details

4.1.1. Preparation of the library

The structures of 55 nitriles and 4888 carboxylic acids, commercially available at Merck database, were used for building the novel library of 1,2,4-oxadiazoles. The reagents were converted from 2D to 3D structures using LigPrep and prepared using Reagent Preparation: the cyano group and the acidic moiety were removed in order to retain only the useful building blocks. The final.bld files were combined with 1,2,4-oxadiazole scaffold obtaining a novel library of 273,728 compounds [36,37]. LigPrep [38] performed calculation increased the number to 303,618 molecules. QikProp [39] and LigFilter were applied and a final library of 150,512 was obtained and submitted to docking studies.

4.1.2. Docking studies

The human crystal structure released in 2017 (PDB code: 5TL9) [40] of mPGES-1 was used to perform structure-based molecular docking experiments. The three-dimensional model of the protein was prepared using the Schrödinger Protein Preparation Wizard [40]: hydrogens and cap termini were added, bond orders were assigned, water molecules were removed. Then, the combinatorial library was submitted to the virtual screening workflow (VSW) using Glide [41] software. The receptor grid adopted for molecular docking calculation was focused onto the co-crystallized ligand binding site [40] characterized from inner- and outer-box dimensions of 10 × 10 × 10 and 27.6 × 27.6 × 27.6, respectively. VSW consisted of three rounds of experiments: 1) High-Throughput Virtual Screening (HTVS) precision mode of Glide for a first enrichment from the starting library of compounds with a high fastness; 2) Standard Precision (SP) for the analysis of the 60% top-ranked poses of HTVS filtered according to docking score values, which overcomes the first step in both sampling and scoring performances; 3) Extra-Precision (XP) for the analysis of the 70% top-ranked poses of SP using the Glide mode experiment, the final and most accurate docking step. Finally, specific filters on 4064 selected docking poses were applied using the pose filter tool of Maestro [40], setting the key interac-

tions as a qualitative filter. Furthermore, the final selection of the most promising molecules was also optimizing considering computational tools: a) SwissADME [47], for filtering the compound displaying the features of "Pan-Assay Interference Compounds"; b) detailed analysis of the other specific pharmaceutically relevant properties obtained by QikProp software [39] (Table S1, Supporting Information).

4.2. Chemistry

1D and 2D NMR spectra were recorded on Bruker Avance NEO 400 spectrometer with an RT-DR-BF/1H-5 mm-OZ SmartProbe (^{1}H at 400 MHz, ^{19}F at 376 MHz and ^{13}C at 100 MHz).

Coupling constants (*J* values) are given in Hertz (Hz), chemical shifts are reported in δ (ppm) and referred to the residual CHD_2OD as internal standards (δ_H = 3.31 e δ_C = 49.0 ppm). All of the recorded signals are in accordance with the proposed structures. Spin multiplicities are given as s (*singlet*), br s (*broad singlet*), d (*doublet*), dd (*doublet of doublets*), t (*triplet*), br t (*broad triplet*) or m (*multiplet*). ESI-MS spectra analysis was carried out on a mass spectrometer LTQ-XL. Specific rotations were measured on a PerkineElmer 243 B polarimeter.

HPLC was performed with a Waters Model 510 pump equipped with Waters Rheodine injector and a differential refractometer, model 401. Reaction progress was monitored via thin layer chromatography (TLC) on Alugram silica gel G/UV254 plates.

The silica gel MN Kiesel gel 60 (70–230 mesh) of Macherey-Nagel was used for flash chromatography. HPLC final purification was performed as detailed in Section 4.2. The purity of compounds was determined to be always greater than 95% by HPLC analysis.

Solvents and reagents were used as supplied from commercial sources with the exception of methanol that was dried as previously reported [29].

All reactions were carried out under argon atmosphere using flame-dried glassware.

Acids **1a** (2-(4-hydroxyphenyl)propionic acid), **2a** (3-(3-hydroxyphenyl)propionic acid), **3a** (4-hydroxymethylphenylacetic acid), **4a** (3-hydroxybenzoic acid), **5a** (3-hydroxy-2,4,5-trifluorobenzoic acid) **6a** [(2*S*, 4*R*)-1-acetyl-4-hydroxypyrrolidine-2-carboxylic acid)], **7a** (indole-4-carboxylic acid) and **10a (**Boc-L-Tyr-OH) are commercially available and are purchased from Sigma Aldrich®. Boc-protected acids **8a** (5-(*tert*-butoxycarbonyl)amino-2-hydroxybenzoic acid), **9a** [(2*R*)-2-(*tert*-butoxycarbonyl)amino-2-(4-hydroxyphenyl)acetic acid] and **11a** (α-methyl-(DL)-Boc-Tyrosine) were synthesized according to the reported methods.

4.2.1. Synthetic procedures for N′-hydroxy-4-(thiophen-3-yl) benzimidamide (13)

Potassium carbonate (1.5 mol eq.) and hydroxylamine chloridrate (2.5 mol eq.) were added to a solution of 4-(3-thiophenyl)benzonitrile **12** (1 mol eq.) in dry methanol. The mixture was refluxed for 8 h in inert atmosphere. The reaction was concentrated under vacuum, diluted with water, and extracted three times with CH_2Cl_2. The organic phases were dried with anhydrous Na_2SO_4, filtrated and concentrated under vacuum to obtain the correspondent amidoxime **13** (70% yield). The product was subjected to the next steps without any purification. ^{1}H NMR (400 MHz, CD_3OD): δ_H 7.91 (2H, d, *J* = 8.5 Hz), 7.77 (2H, d, *J* = 8.5 Hz), 7.69 (2H, m), 7.52 (1H, d, *J* = 1.9 Hz); ^{13}C NMR (100 MHz, CD_3OD): δ_C 161.5, 141.9, 141.8, 133.7129.2 (2C), 128.2, 128.0 (2C), 127.0, 123.7. ESI-MS *m/z* 219.1 $[M + H]^+$.

4.2.2. Synthetic procedures for compounds 1–7

DIPEA (1.8 mol eq.) was added to a solution of carboxylic acids **1a-7a** (1.2 mol eq.) dissolved in DMF dry. HBTU (1.5 mol eq.), was added to the mixture at room temperature as coupling reagent. Amidoxime **13** (1 mol eq.) was added 10 min later. The mixture was stirred at 140 °C for 12 h, then fractionated in water and ethyl acetate for three times. The organic layer was cooled and washed three times with a saturated solution of LiBr, then with a saturated solution of $NaHCO_3$ and distilled water. The organic layer was dried over anhydrous Na_2SO_4, filtered and concentrated under reduced pressure (40–75% yield).

4.2.3. Procedures for Boc protection of acids 8a and 11a

5-amino-2-hydroxybenzoic acid (0.653 mmol, 1 eq) and α-methyl-DL-tyrosine (0.512 mmol, 1 eq) were respectively treated with Boc_2O (2eq) in 10% TEA in MeOH (5 ml) and stirred at rt overnight. Then the reaction solution was concentrated under reduced pressure, and the residue was extracted with H_2O/DCM for three times. Purification on silica gel (DCM:MeOH) afforded Boc-protected acids **8a** and **11a**.

4.2.4. Procedure for Boc protection of acid 9a

D-4-hydroxyphenylglycine (0.597 mmol, 1 eq) was dissolved in a solution of $NaHCO_3$ (1 M) and Boc_2O (2.5 eq) in 1,4-dioxane at 0 °C. The solution was stirred overnight, and after the pH was adjusted until 2–3 using HCl 2 N, it was extracted with H_2O/EtOAc for three times to give Boc-protected acid **9a**.

4.2.5. Synthetic procedures for compounds 8–11

The compounds **8b-11b** were prepared treating the Boc-protected acids **8a**, **9a** and **11a** and the Boc-L-tyrosine **10a** with amidoxime **13** using the same synthetic procedure followed for compounds **1**–**7**.

Boc deprotection using a solution of DCM:TFA (1:1) at rt for 2h afforded the final compounds **8–11**.

5-(1-(4-hydroxyphenyl)ethyl)-3-(4-(thiophen-3-yl)*phenyl)-1,2,4-oxadiazole* **(1).** An analytic sample of crude reaction was purified by HPLC using a Luna Column C-18 (10 μm, 250 mm × 10 mm) with MeOH/H_2O (80:20) as eluent (flow rate 3.00 mL/min) affording compound **1** (t_R = 13.5 min). ^{1}H NMR (400 MHz, CD_3OD): δ_H 8.10 (2H, d, *J* = 8.5 Hz), 7.83 (2H, d, *J* = 8.5 Hz), 7.78 (1H, dd, *J* = 2.7, 1.6 Hz) 7.52 (2H, ovl), 7.22 (2H, d, *J* = 8.6 Hz), 6.79 (2H, d, *J* = 8.6 Hz) 4.46 (1H, q, *J* = 7.2 Hz), 1.76 (3H, d, *J* = 7.2 Hz); ^{13}C NMR (100 MHz, CD_3OD): δ_C 184.0, 169.2, 158.1, 142.5, 139.7, 132.5, 129.7 (2C), 128.8 (2C), 128.0 (3C), 127.4, 126.9, 123.0, 117.0 (2C), 38.8, 20.2; ESI-MS *m/z* 349.1 $[M + H]^+$.

5-(2-(3-hydroxyphenyl)ethyl)-3-(4-(thiophen-3-yl)*phenyl)-1,2,4-oxadiazole* **(2).** An analytic sample of crude reaction was purified by HPLC using Luna Column C-18 (10 μm, 250 mm × 10 mm) with MeOH/H_2O (80:20) as eluent (flow rate 3.00 mL/min) to give compound **2** (t_R = 23.5 min). ^{1}H NMR (400 MHz, CD_3OD): δ_H 8.07 (2H, d, *J* = 8.5 Hz), 7.83 (2H, d, *J* = 8.5 Hz), 7.78 (1H, m), 7.54 (2H, ovl) 7.11 (1H, t, *J* = 7.9 Hz), 6.71 (1H, d, *J* = 7.9 Hz), 6.70 (1H, s), 6.63 (1H, d, *J* = 7.9 Hz), 3.27 (2H, t, *J* = 7.7 Hz), 3.13 (2H, t, *J* = 7.7 Hz); ^{13}C NMR (100 MHz, CD_3OD): δ_C 181.4, 169.2, 159.0, 142.6 (2C), 140.1, 130.5, 129.1 (2C), 127.9 (3C), 127.2, 126.9, 122.8, 120.5, 116.4, 114.7, 33.5, 28.9; ESI-MS *m/z* 349.1 $[M + H]^+$.

5-(4-(hydroxymethyl)benzyl)-3-(4-(thiophen-3-yl)*phenyl)-1,2,4-oxadiazole* **(3).** An analytic sample of crude reaction was purified by HPLC using Luna Column C-18 (10 μm, 250 mm × 10 mm) with MeOH/H_2O (80:20) as eluent (flow rate 3.00 mL/min) to give compound **3** (t_R = 15.5 min). ^{1}H NMR (400 MHz, CD_3OD): δ_H 8.08 (2H, d, *J* = 8.4 Hz), 7.83 (2H, d, *J* = 8.4 Hz), 7.78 (1H, dd, *J* = 2.5, 1.6 Hz), 7.54 (2H, ovl), 7.38 (4H, s), 4.61 (2H, s), 4.36 (2H, s); ^{13}C NMR (100 MHz, CD_3OD): δ_C 180.0, 169.3, 142.5, 142.2, 140.0, 134.3, 130.0 (2C), 128.7 (2C), 128.5 (2C), 127.7 (3C), 126.9, 126.4, 122.6, 64.4, 33.4. ESI MS *m/z* 349.1 $[M + H]^+$.

5-(3-hydroxyphenyl)-3-(4-(thiophen-3-yl)*phenyl)-1,2,4-oxadiazole* **(4).** An analytic sample of crude reaction was purified by HPLC using Luna Column C-18 (10 μm, 250 mm × 10 mm) with MeOH/H_2O (90:10) as eluent (flow rate 3.00 mL/min) to give compound **4** (t_R = 8.0 min). ^{1}H NMR (400 MHz, CD_3OD): δ_H 8.17 (2H, d, *J* = 8.4 Hz), 7.86 (2H, d, *J* = 8.4 Hz), 7.80 (1H, dd, *J* = 2.7,

1.3 Hz), 7.69 (1H, d, J = 7.7 Hz), 7.62 (1H, br t, J = 2.0 Hz), 7.56 (1H, dd, J = 5.0, 1.3 Hz), 7.53 (1H, dd, J = 5.0, 2.7 Hz), 7.43 (1H, t, J = 7.7 Hz), 7.09 (1H, dd, J = 7.7, 2.0 Hz); ^{13}C NMR (100 MHz, CD_3OD): δ_C 177.4, 169.9, 159.6, 142.5, 140.1, 131.6, 129.0 (2C), 127.7 (3C), 127.0, 126.6, 126.4, 122.7, 121.3, 120.1, 115.5. ESI-MS m/z 321.1 $[M + H]^+$.

5-(2,4,5-trifluoro-3-hydroxyphenyl)-3-(4-(thiophen-3-yl*)phenyl)-1,2,4-oxadiazole* **(5).** An analytic sample of crude reaction was purified by HPLC using Luna Column C-18 (10 μm, 250 mm × 10 mm) with MeOH/H_2O (92:8) as eluent (flow rate 3.00 mL/min) to give compound **5** (t_R = 10.5 min). ^{1}H NMR (400 MHz, CD_3OD): δ_H 8.14 (2H, d, J = 8.4 Hz), 7.84 (2H, d, J = 8.4 Hz), 7.77 (1H, dd, J = 2.8, 1.3 Hz), 7.54 (1H, dd, J = 5.0, 1.3 Hz), 7.53 (1H, dd, J = 5.0, 2.8 Hz), 7.49 (1H, m); ^{13}C NMR (100 MHz, CD_3OD): δ_C 173.2, 169.4, 150.1, 147.6, 144.1, 142.4, 140.2, 138.8, 128.7 (2C), 127.9 (2C), 127.5, 127.0, 126.4, 122.4, 109.0, 106.3.^{19}F (376 MHz): δ_F −134.4 (m); −142.5 (m); −150.7 (m). ESI-MS m/z 375.0 $[M + H]^+$.

5-((2S-4R)-1-acetyl-4-hydroxypyrrolidin-2-yl*)-3-(4-(thiophen*-3-yl*)phenyl)-1,2,4-oxadiazole* **(6).** An analytic sample of crude reaction was purified by HPLC using Luna Column C-18 (10 μm, 250 mm × 10 mm) with MeOH/H_2O (68:32) as eluent (flow rate 3.00 mL/min) to give compound **6** (t_R = 11.5 min). ^{1}H NMR (400 MHz, CD_3OD): δ_H 8.05 (2H, d, J = 8.4 Hz), 7.81 (2H, d, J = 8.4 Hz), 7.77 (1H, dd, J = 2.5, 1.5 Hz), 7.54 (2H, ovl), 5.34 (1H, t, J = 8.1 Hz), 4.63 (1H, m), 4.00 (1H, dd, J = 11.0, 4.4 Hz) 3.69 (1H, br d, J = 11.0 Hz), 2.46 (1H, m), 2.28 (1H, m), 2.15 (3H, s); ^{13}C NMR (100 MHz, CD_3OD): δ_C 181.5, 172.7, 169.3, 142.4, 141.1, 128.9 (2C), 127.7 (3C), 127.0, 126.3, 122.7, 70.7, 57.0, 53.6, 40.6, 22.3. $[\alpha]_D^{25}$ − 30.7 (c = 0.22 in MeOH). ESI-MS m/z 356.1 $[M + H]^+$.

5-(1H-indol-4-yl*)-3-(4-(thiophen*-3-yl*)phenyl)-1,2,4-oxadiazole* **(7).** An analytic sample of crude reaction was purified by HPLC using Luna Column C-18 (10 μm, 250 mm × 10 mm) with MeOH/H_2O (95:05) as eluent (flow rate 3.00 mL/min) to give compound **7** (t_R = 9.0 min). ^{1}H NMR (400 MHz, CD_3OD): δ_H 8.24 (2H, d, J = 8.5 Hz), 8.04 (1H, dd, J = 7.8, 0.7 Hz), 7.88 (2H, d, J = 8.5 Hz), 7.80 (1H, dd, J = 2.8, 1.3 Hz), 7.73 (1H, br dd, J = 7.8, 1.3 Hz), 7.57 (1H, dd, J = 5.0, 1.3 Hz), 7.55 (1H, d, J = 3.0 Hz), 7.53 (1H, d, J = 3.0 Hz), 7.33 (1H, d, J = 7.8 Hz) 7.30 (1H, d, J = 5.0, 0.7 Hz); ^{13}C NMR (100 MHz, CD_3OD): δ_C 182.2, 169.7, 142.6, 139.9, 138.6, 129.0 (2C), 128.7, 127.8 (2C), 127.7, 127.4, 127.1, 127.0, 122.7, 122.6, 122.0, 117.5, 115.9, 103.3. ESI-MS m/z 344.1 $[M + H]^+$.

5-(5-amino-2-hydroxyphenyl)-3-(4-(thiophen-3-yl*)phenyl)-1,2,4-oxadiazole* **(8).** An analytic sample of crude reaction was purified by HPLC using Luna Column C-18 (10 μm, 250 mm × 10 mm) with MeOH/H_2O (68:32) + 0.1% TFA as eluent (flow rate 3.00 mL/min) to give compound **8** (t_R = 17.0 min). ^{1}H NMR (400 MHz, CD_3OD): δ_H 8.20 (2H, d, J = 8.6 Hz), 8.00 (1H, dd, J = 2.7 Hz), 7.91 (2H, d, J = 8.6 Hz), 7.84 (1H, dd, J = 2.7 and 1.5 Hz) 7.58 (1H, dd, J = 5.1 amd 1.5 Hz)), 7.57 (1H, dd, J = 5.1 and 2.7 Hz), 7.52 (1H, dd, J = 8.9, 2.7 Hz), 7.28 (1H, d, J = 8.9 Hz) ^{13}C NMR (100 MHz, CD_3OD): δ_C 175.2, 169.1, 158.5, 142.6, 140.8, 139.3, 129.8, 129.0 (2C), 127.9 (2C), 127.7, 126.9, 126.0, 122.9, 122.8, 122.4, 120.3. ESI-MS m/z 336.1 $[M + H]^+$.

(R)-5-(amino(4-hydroxyphenyl)methyl)-3-(4-(thiophen-3-yl*)phenyl)-1,2,4-oxadiazole* **(9).** An analytic sample of crude reaction was purified by HPLC using Luna Column C-18 (10 μm, 250 mm × 10 mm),with MeOH/H_2O (70:30) + 0.1% TFA as eluent (flow rate 3.00 mL/min) to give compound **9** (t_R = 5.0 min). ^{1}H NMR (400 MHz, CD_3OD): δ_H 8.16 (2H, d, J = 8.3 Hz), 7.86 (2H, d, J = 8.3 Hz), 7.80 (1H, dd, J = 2.5, 1.5 Hz), 7.55 (2H, ovl), 7.37 (2H, d, J = 8.5 Hz), 6.91 (2H, d, J = 8.5 Hz), 6.01 (1H, s); ^{13}C NMR (100 MHz, CD_3OD): δ_C 176.8, 169.4, 160.9, 142.3, 140.6, 130.9 (2C), 129.1 (2C), 127.8 (3C), 127.0, 125.5, 122.9, 122.7, 117.4 (2C), 52.2. $[\alpha]_D^{25}$ +17 (c = 0.76 in MeOH). ESI-MS m/z 350.1 $[M + H]^+$.

(S)-5-(1-amino-2-(4-hydroxyphenyl)ethyl)-3-(4-(thiophen-3-yl*)phenyl)-1,2,4-oxadiazole* **(10).** An analytic sample of crude reaction was purified by HPLC using Luna Column C-18 (10 μm, 250 mm × 10 mm, flow rate 3.00 mL/min) using as mobile phase Buffer A (0.1% TFA in water) and Buffer B (0.1% TFA in acetonitrile), with the following gradient: the initial solvent condition was 20% solvent B for 3 min; the gradient was then gradually increased from 20% to 95% solvent B over 18 min; solvent B was increased to 100% and was kept at 100% of B for 10 min. The purification afforded compound **10** (t_R = 14.0 min). ^{1}H NMR (400 MHz, CD_3OD): δ_H 8.11 (2H, d, J = 8.4 Hz), 7.86 (2H, d, J = 8.4 Hz), 7.78 (1H, dd, J = 2.5, 1.7 Hz), 7.55 (2H, ovl), 7.04 (2H, d, J = 8.5 Hz), 6.78 (2H, d, J = 8.5 Hz), 5.05 (1H, t, J = 7.3 Hz), 3.35 (2H, d, J = 7.3); ^{13}C NMR (100 MHz, CD_3OD): δ_C 177.4, 170.6, 159.5, 142.9, 141.2, 131.0 (2C), 129.6 (2C), 128.3, 128.0 (2C), 127.2, 126.0, 125.5, 122.8, 117.4 (2C), 50.8, 38.4. $[\alpha]_D^{25}$ + 38 (c = 0.15 in MeOH). ESI-MS m/z 364.1 $[M + H]^+$.

5-(1-amino-1-methyl-2-(4-hydroxyphenyl)ethyl)-3-(4-(thiophen-3-yl*)phenyl)-1,2,4-oxadiazole* **(11).** An analytic sample of crude reaction was purified by HPLC using Luna Column C-18 (10 μm, 250 mm × 10 mm) with MeOH/H_2O (50:50) + 0.1% TFA as eluent (flow rate 3.00 mL/min) to give compound **11** (t_R = 6.0 min). ^{1}H NMR (400 MHz, CD_3OD): δ_H 7.92 (2H, d, J = 8.4 Hz), 7.91 (1H, ovl), 7.84 (2H, d, J = 8.4 Hz), 7.57 (2H, ovl), 7.00 (2H, d, J = 8.5 Hz), 6.61 (2H, d, J = 8.5 Hz), 3.13 (1H, d, J = 13.9 Hz), 3.07 (1H, d, J = 13.9 Hz), 1.63 (3H, s); ^{13}C NMR (100 MHz, CD_3OD): δ_C 185.1, 169.2, 159.4, 142.9, 142.7, 131.9 (2C), 129.9 (2C), 128.2, 128.0 (2C), 126.9, 126.8, 125.5, 124.5, 115.8 (2C), 70.7, 44.0, 22.6. ESI-MS m/z 378.1 $[M + H]^+$.

4.3. Pharmacology

4.3.1. Human leukocytes and A549 cells

Human neutrophils and monocytes were freshly isolated from leukocyte concentrates obtained from the Institute of Transfusion Medicine, University Hospital Jena. Donors were healthy adult volunteers and gave written consent, after they were informed about the aim of the study. Also, the ethical commission of the University Hospital in Jena approved the protocol for experiments, and all methods were performed in accordance with the relevant guidelines and regulations. Briefly, neutrophils were isolated [61] by dextran sedimentation, centrifugation on lymphocyte separation medium (LSM 1077, PAA, Coelbe, Germany) and hypotonic lysis of erythrocytes. Neutrophils were resuspended in PBS containing glucose (0.1%) to a final cell density of 5 × 10^6 cells/ml. Monocytes were separated from peripheral blood mononuclear cells (PBMC) by adherence to cell culture flasks (Greiner Bio-one, Nuertingen, Germany) for 1.5 h (37 °C, 5% CO_2) in RPMI 1640 containing L-glutamine (1 mM), heat-inactivated FCS (10%), penicillin (100 U/mL) and streptomycin (100 μg/mL), followed by cell-scraping and resuspension in PBS.

Human lung carcinoma A549 cells were purchased from Cell Application Inc., Sigma-Aldrich, Merck (Darmstadt, Germany) and maintained in DMEM supplemented with 10% heat-inactivated fetal bovine serum (Invitrogen, Carslbad, CA, USA), in a 5% CO_2 humid atmosphere. To ensure logarithmic growth, the cells were subcultured every 2 days. The cell line was tested for mycoplasma using PCR analysis.

4.3.2. Cell viability assay on A549 cell line

The viability of A549 cells after incubation with test compounds was determined by MTT conversion assay. Briefly, the cells (2 × 10^4) were seeded in triplicate in 96 well/plates and incubated with compound **5** (10 μM) and or DMSO 0.1% (v/v) for 48 h in DMEM (37 °C, 5% CO_2). MTT (5 mg/mL) was added and after 1 h (37 °C, 5% CO_2) the

medium was replaced with DMSO (100 μL per well). Finally, formazan formation was detected by measurement of absorbance at 570 nm.

4.3.3. Cell viability assay on monocytes

Acute cytotoxicity of compound **5** was analyzed in isolated human monocytes. Cells (0.2×10^6 per well) were seeded in 100 μL buffer on 96-well plates and treated with the test compounds (10 μM), triton (0.1%, positive control) or vehicle (0.5% DMSO) over 24 h (37 °C, 5% CO_2). MTT (5 mg/mL) was added and after 2 h (37 °C, 5% CO_2) cells were lysed by SDS treatment (10%, pH 4.5). After 17 h, formazan formation was detected by measurement of absorbance at 570 nm.

4.3.4. Determination of 5-LO products in intact cells

Freshly isolated neutrophils were resuspended in 1 mL PBS buffer containing 0.1% glucose and 1 mM $CaCl_2$ to a final cell density of 5×10^6/mL. Cells were pre-incubated with test compounds or DMSO vehicle (0.1%) at 37 °C for 10 min. Then, 2.5 μM Ca^{2+}-ionophore A23187 with or without supplementation of 20 μM AA was added as stimulus, and cells were left at 37 °C for 10 min. 5-LO product formation was stopped on ice, after the addition of 1 mL ice-cold methanol, and 530 μl acidified PBS and PGB_1 as internal standard were added. Afterwards, cells were centrifuged ($2000 \times g$, 10 min, rt) and supernatants were submitted to solid phase extraction. 5-LO product formation (LTB_4 and its trans isomers and 5HETE) was quantified by RP-HPLC as described elsewhere [62].

4.3.5. Cell-free mPGES-1 activity assay

The mPGES-1 was obtained from microsomes of A549 cells stimulated with IL-1β (1 ng/ml) for 48 h. Cells were sonicated and the homogenate was submitted to differential centrifugation at $10{,}000 \times g$ for 10 min and $174{,}000 \times g$ for 1 h at a temperature of 4 °C. The pellet (microsomal fraction) was resuspended in 1 ml homogenization buffer (0.1 M potassium phosphate buffer, pH 7.4, 1 mM phenylmethanesulphonyl fluoride, 60 μg/mL soybean trypsin inhibitor, 1 μg/mL leupeptin, 2.5 mM glutathione, and 250 mM sucrose), the total protein concentration was determined, and microsomes were diluted in potassium phosphate buffer (0.1 M, pH 7.4) containing glutathione (2.5 mM) and seeded in a 96-well plate. Test compounds or DMSO (1%) were added, and preincubated for 15 min on ice, and the reactions was started by adding 20 μM of PGH_2. After 1 min, 100 μl of a stop solution (40 mM $FeCl_3$, 80 mM citric acid, and 10 μM 11β-PGE_2) were added. PGE_2 and 11β-PGE_2 were extracted by solid-phase extraction, and RP-HPLC was used to quantify the product formation, as previously described [63].

4.3.6. Cell-free 5-LO activity assay

Human recombinant 5-LO was expressed in *E.coli* BL21 transformed with pT3-5-LO plasmid at 30 °C overnight as described before [64]. The cells were lysed in a buffer containing triethanolamine (50 mM, pH 8.0), EDTA (5 mM), phenylmethanesulphonyl fluoride (1 mM), soybean trypsin inhibitor (60 μg/mL), dithiothreitol (2 mM) and lysozyme (1 mg/mL) by sonification (3×15 s). Then, a centrifugation step was performed ($40{,}000 \times g$, 20 min, 4 °C) and the supernatant was collected. The 5-LO enzyme was purified by affinity chromatography using an ATP-agarose column and diluted with PBS buffer containing 1 mM EDTA. Afterwards, 0.5 μg purified 5-LO in 1 mL PBS plus 1 mM EDTA was pre-incubated with the test compounds or vehicle (0.1% DMSO) on ice for 10 min and then stimulated with 20 μM AA and 2 mM $CaCl_2$ for 10 min at 37 °C. Ice-cold methanol (1 mL) was added to stop the reactions, and 530 μl acidified PBS and PGB_1 as internal standard were added, and solid phase extraction of 5-LO products (trans isomers of LTB_4 and 5HETE) was performed using C18 RP-columns (100 mg, UCT, Bristol, PA, USA). 5-LO products were analyzed by RP-HPLC as previously described [62].

4.3.7. Cell-free COXs activity assay

Isolated ovine COX-1 and recombinant human COX-2, respectively, were used for the evaluation of the activity of compound **5** on cyclooxygenases. COXs were diluted in Tris buffer (100 mM, pH 8) supplemented with glutathione (5 mM), EDTA (100 μM) and hemoglobin (5 μM) to a final concentration of 50 U/mL for COX-1 and 20 U/mL for COX-2, and pre-incubated with test compounds or vehicle (0.1% DMSO) for 5 min at room temperature. After 1 min at 37 °C, reactions were started adding arachidonic acid to a final concentration of 5 μM for COX-1 and 2 μM for COX-2. After 5 min at 37 °C, 1 mL of ice-cold methanol was added and the reactions were stopped on ice. Internal PGB_1 standard and 530 μl acidified PBS were added, solid phase extraction was performed, and COX product formation was determined using RP-HPLC by analysis of 12-HHT formation [65–67].

4.3.8. Expression, purification and activity assay of human recombinant sEH

Human recombinant sEH was expressed and purified as reported before [36]. In brief, Sf9 cells were infected with a recombinant baculovirus, provided by Dr. B. Hammock, University of California, Davis, CA. After 72 h, cells were pelleted and sonicated (3×10 s at 4 °C) in lysis buffer containing $NaHPO_4$ (50 mM, pH 8), NaCl (300 mM), glycerol (10%), EDTA (1 mM), phenylmethanesulphonyl fluoride (1 mM), leupeptin (10 μg/mL), and soybean trypsin inhibitor (60 μg/mL). A centrifugation ($100{,}000 \times g$, 60 min, 4 °C) was applied, and supernatants were collected and applied to benzylthio-sepharose-affinity chromatography in order to purify sEH by elution with 4-fluorochalcone oxide in PBS containing DTT (1 mM) and EDTA (1 mM). Dialyzed and concentrated (Millipore Amicon-Ultra-15 centrifugal filter) enzyme solution was assayed for total protein with Bio-Rad protein detection kit (Bio-Rad Laboratories, Munich, Germany) and the activity of sEH was determined by using a fluorescence-based assay as described before [66,67]. Thus, sEH was diluted in Tris buffer (25 mM, pH 7) supplemented with BSA (0.1 mg/mL) to an appropriate enzyme concentration and pre-incubated with compound **5** (10 μM) or vehicle (0.1% DMSO) for 15 min at room temperature. The reaction was started by addition of 50 μM 3-phenyl-cyano(6-methoxy-2-naphthalenyl)methyl ester-2-oxiraneacetic acid (PHOME), a non-fluorescent compound that is enzymatically converted into fluorescent 6-methoxy-naphtaldehyde at rt. After 60 min, the reaction was stopped by $ZnSO_4$ (200 mM) and fluorescence was detected (λ_{em} 465 nm, λ_{ex} 330 nm).

4.3.9. Animals

Male CD-1 mice (10–14 weeks of age, 25–30 g of weight) were obtained from Charles River (Milan, Italy) and kept in an animal care facility under controlled temperature, humidity, and on a 12 h:12 h light: dark cycle, with *ad libitum* access to water and standard laboratory chow diet. All experimental procedures were carried out according to the international and national law and policies (EU Directive 2010/63/EU for animal experiments, ARRIVE guidelines, and the Basel declaration including the 3R concept) [68,69]. All procedures were carried out to minimize the number of animals ($n = 6$ per group) and their suffering.

4.3.10. Induction of peritonitis in mice

To examine the anti-inflammatory action of compound **5**, mice were randomly divided into different experimental groups: control group (Ctrl), model group (zymosan + vehicle compound **5**), zymosan + compound **5** (0.1, 1, and 10 mg/kg), and zymosan + dexamethasone (3 mg/kg) group. Animals received the selected compound or dexamethasone intraperitoneally (i.p.) 30 min after i.p. injection of zymosan (500 mg/kg) [53–55]. Ctrl and model group received an equal volume of vehicle (PBS or DMSO/saline 1:3, respectively) according to the same schedule. Peritonitis was induced in mice as previously described [53,55]. In brief, 500 mg/kg of zymosan A were dissolved in

PBS and then boiled before the i.p. injection (0.5 mL). Peritoneal exudates were collected at selected time points (4 and 24 h) by washing the cavity with 2 mL of PBS. Then cell number of lavage fluids was determined by TC10 automated cell counter (Bio-Rad, Milan, Italy) using disposable slides, TC10 trypan blue dye (0.4% trypan blue dye w/v in 0.81% sodium chloride and 0.06% potassium phosphate dibasic solution), and a CCD camera to count cells based on the analyses of captured images. The remaining lavage fluids were centrifuged at 3000 rpm for 20 min at 4 °C, and supernatants were frozen at −80 °C for further ELISA analysis [55]. Dexamethasone and zymosan A were purchased from Sigma-Aldrich (Milan, Italy). DMSO was purchased from Merck (Italy). Unless otherwise stated, all the other reagents were purchased from Carlo Erba (Milan, Italy).

4.3.11. Enzyme-linked immunosorbent assay (ELISA)

The levels of IL-1β, IL-6, IL-10 and TNF-α in the peritoneal exudates at 4 and 24 h were measured using commercially available ELISA kits (eBioscience Co., San Diego, CA, USA) according to the manufacturer instructions. Briefly, 100 μL of peritoneal exudates, diluted standards, quality controls, and dilution buffer (blank) were applied on a precoated plate with the monoclonal antibody for 2 h. After washing, 100 μL of biotin-labeled antibody was added and incubation continued for 1 h. The plate was washed and 100 μL of the streptavidin–HRP conjugate was added, and the plate was incubated for a further 30 min period in the dark. The addition of 100 μL of the substrate and stop solution represented the last steps before the reading of absorbance (measured at 450 nm) on a microplate reader [70,71].

4.4. Statistical analysis

The data and statistical analysis in this study comply with the international recommendations on experimental design and analysis in pharmacology [69] and data sharing and presentation in preclinical pharmacology [72,73]. The results obtained were expressed as the mean ± S.D. or as mean ± S.E.M., as reported in the figure legends. IC_{50} values were calculated by nonlinear regression using GraphPad Prism Version 6 software (San Diego, CA) one site binding competition. Statistical evaluation of the data was performed by one-way ANOVA followed by a Bonferroni post hoc test for multiple comparison. GraphPad Prism 8.0 software (San Diego, CA, USA) was used for analysis. Differences between means were considered statistically significant when $P \leq 0.05$ was achieved. Sample size was chosen to ensure alpha 0.05 and power 0.8. Animal weight was used for randomization and group allocation to reduce unwanted sources of variations by data normalization. No animals and related ex vivo samples were excluded from the analysis. *In vivo* studies were carried out to generate groups of equal size (n = 6 of independent values), using randomization and blinded analysis.

Funding sources

The research leading to these results has received funding from AIRC under IG 2018 - ID. 21397 project – P.I. Bifulco Giuseppe from Ministero dell'Università e della Ricerca (MIUR) under PRIN.

2017 (2017A95NCJ) Stolen molecules "Stealing natural products from the depot and reselling them as new drug candidates", and by Deutsche Forschungsgemeinschaft (DFG, German Research Foundation) [project number 316213987, SFB 1278 PolyTarget (projects A04, C02)]. A.S. and M. S. are supported by MIUR Ph.D. scholarship.

Declaration of competing interest

The authors declare that they have no known competing financial interests or personal relationships that could have appeared to influence the work reported in this paper.

Appendix A. Supplementary data

Supplementary data to this article can be found online at https://doi.org/10.1016/j.ejmech.2021.113693.

References

[1] G.J. Martinez-Colon, B.B. Moore, Pharmacol. Ther. 185 (2018) 135–146.
[2] M. Murakami, H. Naraba, T. Tanioka, N. Semmyo, Y. Nakatani, F. Kojima, T. Ikeda, M. Fueki, A. Ueno, S. Oh, I. Kudo, J. Biol. Chem. 275 (2000) 32783–32792.
[3] F. Bergqvist, R. Morgenstern, P.-J. Jakobsson, Prostag. Other Lipid Mediat. 147 (2020) 106383.
[4] M. Korotkova, P.J. Jakobsson, Front. Pharmacol. 1 (2010) 146.
[5] M. Nakanishi, V. Gokhale, E.J. Meuillet, D.W. Rosenberg, Biochimie 92 (2010) 660–664.
[6] M. Nakanishi, D.W. Rosenberg, Semin. Immunopathol. 35 (2013) 123–137.
[7] P. Nandi, G.V. Girish, M. Majumder, X. Xin, E. Tutunea-Fatan, P.K. Lala, BMC Canc. 17 (2017) 11.
[8] A. Koeberle, O. Werz, Biochem. Pharmacol. 98 (2015) 1–15.
[9] A.V. Sampey, S. Monrad, L.J. Crofford, Arthritis Res. Ther. 7 (2005) 114.
[10] J. Ke, Y. Yang, Q. Che, F. Jiang, H. Wang, Z. Chen, M. Zhu, H. Tong, H. Zhang, X. Yan, X. Wang, F. Wang, Y. Liu, C. Dai, X. Wan, Tumour Biol 37 (2016) 12203–12211.
[11] J.W. Meadows, A.L. Eis, D.E. Brockman, L. Myatt, J. Clin. Endocrinol. Metab. 88 (2003) 433–439.
[12] P.J. Jakobsson, R. Morgenstern, J. Mancini, A. Ford-Hutchinson, B. Persson, Protein Sci. 8 (1999) 689–692.
[13] D. Riendeau, R. Aspiotis, D. Ethier, Y. Gareau, E.L. Grimm, J. Guay, S. Guiral, H. Juteau, J.A. Mancini, N. Methot, J. Rubin, R.W. Friesen, Bioorg. Med. Chem. Lett 15 (2005) 3352–3355.
[14] Z.T. Gür, B. Çalışkan, U. Garscha, A. Olgaç, U.S. Schubert, J. Gerstmeier, O. Werz, E. Banoglu, Eur. J. Med. Chem. 150 (2018) 876–899.
[15] M.G. Chini, A. Giordano, M. Potenza, S. Terracciano, K. Fischer, M.C. Vaccaro, E. Colarusso, I. Bruno, R. Riccio, A. Koeberle, O. Werz, G. Bifulco, ACS Med. Chem. Lett. 11 (2020) 783–789.
[16] S. Di Micco, S. Terracciano, V. Cantone, K. Fischer, A. Koeberle, A. Foglia, R. Riccio, O. Werz, I. Bruno, G. Bifulco, Eur. J. Med. Chem. 143 (2018) 1419–1427.
[17] M.G. Chini, C. Ferroni, V. Cantone, P. Dambruoso, G. Varchi, A. Pepe, K. Fischer, C. Pergola, O. Werz, I. Bruno, R. Riccio, G. Bifulco, MedChemComm 6 (2015) 75–79.
[18] G. Lauro, V. Cantone, M. Potenza, K. Fischer, A. Koeberle, O. Werz, R. Riccio, G. Bifulco, MedChemComm 9 (2018) 2028–2036.
[19] M. Iranshahi, M.G. Chini, M. Masullo, A. Sahebkar, A. Javidnia, M. Chitsazian Yazdi, C. Pergola, A. Koeberle, O. Werz, C. Pizza, S. Terracciano, S. Piacente, G. Bifulco, J. Nat. Prod. 78 (2015) 2867–2879.
[20] K. Meirer, D. Steinhilber, E. Proschak, Basic Clin. Pharmacol. Toxicol. 114 (2014) 83–91.
[21] A. Koeberle, O. Werz, Biotechnol. Adv. 36 (2018) 1709–1723.
[22] M.G. Chini, R. De Simone, I. Bruno, R. Riccio, F. Dehm, C. Weinigel, D. Barz, O. Werz, G. Bifulco, Eur. J. Med. Chem. 54 (2012) 311–323.
[23] G. Lauro, S. Terracciano, V. Cantone, D. Ruggiero, K. Fischer, S. Pace, O. Werz, I. Bruno, G. Bifulco, ChemMedChem 15 (2020) 481–489.
[24] E. Durgashivaprasad, G. Mathew, S. Sebastian, S.A. Reddy, J. Mudgal, G.K. Nampurath, Indian J. Pharmacol. 46 (2014) 521–526.
[25] C.S. de Oliveira, B.F. Lira, J.M. Barbosa-Filho, J.G. Lorenzo, P.F. de Athayde-Filho, Molecules 17 (2012) 10192–10231.
[26] G. Verma, M.F. Khan, W. Akhtar, M.M. Alam, M. Akhter, M. Shaquiquzzaman, Mini Rev. Med. Chem. 19 (2019) 477–509.
[27] S. Bajaj, V. Asati, J. Singh, P.P. Roy, Eur. J. Med. Chem. 97 (2015) 124–141.
[28] F.S. Di Leva, C. Festa, A. Carino, S. De Marino, S. Marchianò, D. Di Marino, C. Finamore, M.C. Monti, A. Zampella, S. Fiorucci, V. Limongelli, Sci. Rep. 9 (2019).
[29] C. Festa, C. Finamore, S. Marchianò, F.S. Di Leva, A. Carino, M.C. Monti, F. del Gaudio, S. Ceccacci, V. Limongelli, A. Zampella, S. Fiorucci, S. De Marino, ACS Med. Chem. Lett. 10 (2019) 504–510.
[30] G. Chawla, Mini Rev. Med. Chem. 18 (2018) 1536–1547.
[31] Y.-Y. Zhang, Q.-Q. Zhang, J. Zhang, J.-L. Song, J.-C. Li, K. Han, J.-T. Huang, C.-S. Jiang, H. Zhang, Bioorg. Med. Chem. Lett 30 (2020).
[32] S. Yatam, S.S. Jadav, R. Gundla, K.P. Gundla, G.M. Reddy, M.J. Ahsan, J. Chimakurthy, Chemistry 3 (2018) 10305–10310.
[33] M. Vijaya Bhargavi, P. Shashikala, M. Sumakanth, C. Krishna, Russ. J. Gen. Chem. 88 (2018) 804–811.
[34] S. Yatam, R. Gundla, S.S. Jadav, N.r. Pedavenkatagari, J. Chimakurthy, N. Rani B, T. Kedam, J. Mol. Struct. 1159 (2018) 193–204.
[35] P. Mukherjee, H. Li, I. Sevrioukova, G. Chreifi, P. Martásek, L.J. Roman, T.L. Poulos, R.B. Silverman, J. Med. Chem. 58 (2014) 1067–1088.
[36] R.N. Wixtrom, M.H. Silva, B.D. Hammock, Anal. Biochem. 169 (1988) 71–80.
[37] CombiGlide, L.L.C. Schrödinger, New York, NY (2017).
[38] S. LigPrep, LLC, New York, NY (2017).
[39] S. QikProp, LLC, New York, NY (2017).
[40] K.M. Partridge, S. Antonysamy, S.N. Bhattachar, S. Chandrasekhar, M.J. Fisher, A. Fretland, K. Gooding, A. Harvey, N.E. Hughes, S.L. Kuklish, J.G. Luz, P.R. Manninen, J.E. McGee, D.R. Mudra, A. Navarro, B.H. Norman, S.J. Quimby, M.A. Schiffler, A.V. Sloan, A.M. Warshawsky, J.M. Weller, J.S. York, X.-P. Yu, Bioorg. Med. Chem. Lett 27 (2017) 1478–1483.
[41] S. Glide, LLC, New York, NY (2017).

[42] J.G. Luz, S. Antonysamy, S.L. Kuklish, B. Condon, M.R. Lee, D. Allison, X.-P. Yu, S. Chandrasekhar, R. Backer, A. Zhang, M. Russell, S.S. Chang, A. Harvey, A.V. Sloan, M.J. Fisher, J. Med. Chem. 58 (2015) 4727–4737.
[43] T. Sjogren, J. Nord, M. Ek, P. Johansson, G. Liu, S. Geschwindner, Proc. Natl. Acad. Sci. U. S. A. 110 (2013) 3806–3811.
[44] M.A. Schiffler, S. Antonysamy, S.N. Bhattachar, K.M. Campanale, S. Chandrasekhar, B. Condon, P.V. Desai, M.J. Fisher, C. Groshong, A. Harvey, M.J. Hickey, N.E. Hughes, S.A. Jones, E.J. Kim, S.L. Kuklish, J.G. Luz, B.H. Norman, R.E. Rathmell, J. R. Rizzo, T.W. Seng, S.J. Thibodeaux, T.A. Woods, J.S. York, X.P. Yu, J. Med. Chem. 59 (2016) 194–205.
[45] S.L. Kuklish, S. Antonysamy, S.N. Bhattachar, S. Chandrasekhar, M.J. Fisher, A.J. Fretland, K. Gooding, A. Harvey, N.E. Hughes, J.G. Luz, P.R. Manninen, J.E. McGee, A. Navarro, B.H. Norman, K.M. Partridge, S.J. Quimby, M.A. Schiffler, A.V. Sloan, A. M. Warshawsky, J.S. York, X.P. Yu, Bioorg. Med. Chem. Lett 26 (2016) 4824–4828.
[46] T. Weinert, V. Olieric, S. Waltersperger, E. Panepucci, L. Chen, H. Zhang, D. Zhou, J. Rose, A. Ebihara, S. Kuramitsu, D. Li, N. Howe, G. Schnapp, A. Pautsch, K. Bargsten, A.E. Prota, P. Surana, J. Kottur, D.T. Nair, F. Basilico, V. Cecatiello, S. Pasqualato, A. Boland, O. Weichenrieder, B.C. Wang, M.O. Steinmetz, M. Caffrey, M. Wang, Nat. Methods 12 (2015) 131–133.
[47] A. Daina, O. Michielin, V. Zoete, Sci. Rep. 7 (2017) 42717.
[48] A. Koeberle, U. Siemoneit, U. Buehring, H. Northoff, S. Laufer, W. Albrecht, O. Werz, J. Pharmacol. Exp. Therapeut. 326 (2008) 975–982.
[49] J. Gerstmeier, C. Weinigel, S. Rummler, O. Rådmark, O. Werz, U. Garscha, Faseb. J. 30 (2015) 276–285.
[50] A. Pannunzio, M. Coluccia, Pharmaceuticals (2018) 11.
[51] N.A. Meanwell, J. Med. Chem. 61 (2018) 5822–5880.
[52] S. Cuzzocrea, A. Filippelli, B. Zingarelli, M. Falciani, A.P. Caputi, F. Rossi, Shock 7 (1997) 351–357.
[53] R. Bellavita, F. Raucci, F. Merlino, M. Piccolo, M.G. Ferraro, C. Irace, R. Santamaria, A.J. Iqbal, E. Novellino, P. Grieco, N. Mascolo, F. Maione, Biomed. Pharmacother. 123 (2020).
[54] B.E. Chatterjee, S. Yona, G. Rosignoli, R.E. Young, S. Nourshargh, R.J. Flower, M. Perretti, J. Leukoc. Biol. 78 (2005) 639–646.
[55] F. Raucci, A. Saviano, G.M. Casillo, M. Guerra-Rodriguez, A.A. Mansour, M. Piccolo, M.G. Ferraro, E. Panza, V. Vellecco, C. Irace, F. Caso, R. Scarpa, N. Mascolo, M. Alfaifi, A.J. Iqbal, F. Maione, Br. J. Pharmacol. (2021).
[56] F. D'Acquisto, F. Maione, M. Pederzoli-Ribeil, Biochem. Pharmacol. 79 (2010) 525–534.
[57] S. Liu, J. Zhang, Q. Pang, S. Song, R. Miao, W. Chen, Y. Zhou, C. Liu, Shock 45 (2016) 209–219.
[58] K.W. Moore, R. de Waal Malefyt, R.L. Coffman, A. O'Garra, Annu. Rev. Immunol. 19 (2001) 683–765.
[59] J.M. Schwab, N. Chiang, M. Arita, C.N. Serhan, Nature 447 (2007) 869–874.
[60] J.L. Cash, G.E. White, D.R. Greaves, Chapter 17 zymosan-induced peritonitis as a simple experimental system for the study of inflammation, in: Chemokines, B. Part (Eds.), 2009, pp. 379–396.
[61] A. Boyum, Scand. J. Clin. Lab. Invest. Suppl. 97 (1968) 77–89.
[62] L. Fischer, M. Hornig, C. Pergola, N. Meindl, L. Franke, Y. Tanrikulu, G. Dodt, G. Schneider, D. Steinhilber, O. Werz, Br. J. Pharmacol. 152 (2007) 471–480.
[63] A. Koeberle, U. Siemoneit, U. Buhring, H. Northoff, S. Laufer, W. Albrecht, O. Werz, J. Pharmacol. Exp. Therapeut. 326 (2008) 975–982.
[64] L. Fischer, D. Szellas, O. Rådmark, D. Steinhilber, O. Werz, 17 (2003) 1-24.
[65] D. Albert, I. Zundorf, T. Dingermann, W.E. Muller, D. Steinhilber, O. Werz, Biochem. Pharmacol. 64 (2002) 1767–1775.
[66] U. Garscha, E. Romp, S. Pace, A. Rossi, V. Temml, D. Schuster, S. König, J. Gerstmeier, S. Liening, M. Werner, H. Atze, S. Wittmann, C. Weinigel, S. Rummler, G.K. Scriba, L. Sautebin, O. Werz, Sci. Rep. 7 (2017) 9398.
[67] B. Waltenberger, U. Garscha, V. Temml, J. Liers, O. Werz, D. Schuster, H. Stuppner, J. Chem. Inf. Model. 56 (2016) 747–762.
[68] C. Kilkenny, W. Browne, I.C. Cuthill, M. Emerson, D.G. Altman, Br. J. Pharmacol. 160 (2010) 1577–1579.
[69] M.J. Curtis, R.A. Bond, D. Spina, A. Ahluwalia, S.P.A. Alexander, M.A. Giembycz, A. Gilchrist, D. Hoyer, P.A. Insel, A.A. Izzo, A.J. Lawrence, D.J. MacEwan, L.D.F. Moon, S. Wonnacott, A.H. Weston, J.C. McGrath, Br. J. Pharmacol. 172 (2015) 3461–3471.
[70] F. Maione, A.J. Iqbal, F. Raucci, M. Letek, M. Bauer, F. D'Acquisto, Front. Immunol. 9 (2018).
[71] V. Baradaran Rahimi, H. Rakhshandeh, F. Raucci, B. Buono, R. Shirazinia, A. Samzadeh Kermani, F. Maione, N. Mascolo, V.R. Askari, Molecules 24 (2019).
[72] S.P.H. Alexander, R.E. Roberts, B.R.S. Broughton, C.G. Sobey, C.H. George, S.C. Stanford, G. Cirino, J.R. Docherty, M.A. Giembycz, D. Hoyer, P.A. Insel, A.A. Izzo, Y. Ji, D.J. MacEwan, J. Mangum, S. Wonnacott, A. Ahluwalia, Br. J. Pharmacol. 175 (2018) 407–411.
[73] C.H. George, S.C. Stanford, S. Alexander, G. Cirino, J.R. Docherty, M.A. Giembycz, D. Hoyer, P.A. Insel, A.A. Izzo, Y. Ji, D.J. MacEwan, C.G. Sobey, S. Wonnacott, A. Ahluwalia, Br. J. Pharmacol. 174 (2017) 2801–2804.